IEEE Access
Multidisciplinary | Rapid Review | Open Access Journal

Received 7 March 2024, accepted 21 March 2024, date of publication 25 March 2024, date of current version 29 March 2024.

Digital Object Identifier 10.1109/ACCESS.2024.3381492

RESEARCH ARTICLE

A Novel Remaining Useful Life Prediction Approach Combined eXtreme Gradient Boosting and Multi-Quantile Recurrent Neural Network

YANTAO YIN[1], JIANYIN ZHAO[1], XIAO ZHANG[2], AND YING LIU[3]
[1]No. 3 Department, Naval Aviation University, Yantai 264001, China
[2]College of Artificial Intelligence, Tianjin University of Science and Technology, Tianjin 300457, China
[3]School of Management, Tianjin University of Technology, Tianjin 300384, China

Corresponding author: Ying Liu (liu@email.tjut.edu.cn)

This work was supported in part by the Social Sciences Foundation of the Ministry of Education (Youth Fund) under Grant 18YJC630108, in part by the Scientific Research Project of Tianjin Education Commission under Grant 2019KJ233, and in part by the Research Initiation Fund of Tianjin University of Technology under Grant 01002301.

ABSTRACT Remaining useful life (RUL) prediction is a key technology to ensure the reliability and safety of high-end equipment. Deep learning is widely used for RUL prediction due to the excellent feature extraction ability and nonlinear fitting ability. Traditional recurrent neural networks adopt recursive strategy, which easily lead to the problems of error accumulation and low stability. On the other hand, most deep learning methods are used for point prediction and cannot quantify uncertainty in the prediction results. Although some probability prediction methods based on deep learning can provide probability prediction results, it require the assumption that the prediction results follow a specific distribution in advance. However, the distribution of most prediction results does not match a suitable distribution function. To solve above problems, a novel RUL prediction approach based on eXtreme gradient boosting (XGBoost) and multi-quantile recursive neural network (MQ-RNN) is proposed in this article. Specifically, XGBoost is used to select features closely related to RUL, and the selected features are fed into MQ-RNN to train the RUL prediction model. The advantage of MQ-RNN is that it has non-parametric framework, prediction results can be obtained by multi-quantile regression, which does not require prior assumptions about the distribution of predicted results. Furthermore, the proposed framework is verified by C-MAPSS dataset. Finally, comparative experiments are conducted. The experimental results show that the proposed method maintains good predictive performance in both point estimation and interval estimation.

INDEX TERMS Remaining useful life, eXtreme gradient boosting, multi-quantile recursive neural network, quantile regression, forking sequences training scheme.

I. INTRODUCTION

Prognostics Health Management (PHM) technology is an effective solution to ensure the safety and reliability of high-end equipment [1]. As the key technology of PHM, RUL prediction can warn failures as early as possible to avoid accidents and reduce economic losses [2]. There are two main methods for RUL prediction: physical model-based methods and data-driven methods [3]. Physical model-based methods mainly constructs a parameterized mathematical model describing the degradation process of systems based on the failure mechanism, and updates the mechanism model parameters based on state monitoring data to achieve the RUL [4], [5]. However, due to the complex and diverse fault mechanism of complex systems, it is difficult to establish an accurate physical model [6]. Data-driven prediction

The associate editor coordinating the review of this manuscript and approving it for publication was Jiajie Fan.

methods can be divided into statistical model-based methods and machine learning-based methods [7]. Statistical model-based methods is based on the theory of probability and statistics, using random models to establish monitoring data and infer RUL, which can obtain the probability distribution of RUL [8]. Machine learning-based methods involve analyzing, training and processing the acquired historical data to predict system RUL [9].

In recent years, machine learning-based methods have become the preferred technology for RUL prediction, which can be divided into shallow machine learning prediction methods and deep learning prediction methods [10]. Shallow machine learning prediction methods for RUL prediction include support vector machine [11], extreme learning machine [12], random forest [13], etc. Although shallow neural network training is relatively easy, however, the network structure is simple, and RUL prediction based on shallow machine learning rely on prior knowledge of experts and and signal processing techniques. In addition, it is difficult to automatically analyze and process a large number of monitoring data, resulting in low prediction accuracy and poor robustness.

Deep learning have more powerful feature extraction and nonlinear relationship learning ability than shallow machine learning prediction methods [14], [15], [16], therefore, it is widely used for RUL prediction. For example, Ma et al. [17] used stacked sparse autoencoder to automatically extract performance degradation features from multiple sensors on the aircraft engine, and applied logistic regression to predict the RUL. However, when stacked sparse autoencoder process high-dimensional raw monitoring data, they still need to use various signal processing techniques to extract system degradation indicators. Jiao et al. [18] proposed a RUL prediction method based on deep belief network (DBN), and Ren et al. [19] proposed a RUL prediction method based on deep convolutional neural network (CNN). However, DBN and CNN are mainly used for feature extraction, which should be combined with other methods to predict RUL. Then Guo et al. [20] utilized RNN to predict RUL of the bearing, but RNN can cause the problems of gradient vanishing and gradient explosion.Long Short Time Memory(LSTM)and Gated Recurrent Neural Network (GRU) can overcome these shortcomings. Then Ding et al. [21] applied the LSTM neural network model to predict RUL of bearings. Behera et al. [22] used multi-scale depth bidirectional gated recurrent neural network (MDBGRU) to predict the RUL of aero engines, which can simultaneously capture the dependency of multiple time scales and improve the accuracy and expressiveness of sequence data processing. The above deep learning prediction methods, especially those based on recursive prediction, have the problem of error accumulation, and the existing models still have the problem of low stability in training.

To improve the RUL prediction accuracy, more and more researchers integrate multiple methods to compensate for the shortcomings of a single deep learning network. For instance, Xiang et al. [23] proposed a RUL prediction model for aeroengines by combining multicellular LSTM neural network and DNN. Qin et al. [24] proposed a degradation trend-constrained variational autoencoder to construct an health indicator (HI) vector with obvious degradation trend, and the constructed HI was used to predict the corresponding RUL using macro-microattention-based long-term short-term memory (MMALSTM). Zhou et al. [25] explored a new dual-threaded gated cycle unit (DTGRU) in order to improve its ability to predict complex degradation trajecues. Zhou et al. [26] innovatively constructed the Distributed Contact Ratio Measure Health Indicator (DCRHI), then the combined memory gated cycle unit (CMGRU) was used to predict the RUL of the bearing. Li et al. [27] proposed a RUL prediction method combining multi-branch improved Convolutional network (MBCNN) and bidirectional Long short-term memory (BiLSTM) network to solve the problem of low prediction accuracy due to difficulty in feature extraction of bearing data. Jiang et al. [28] designed a combined time convolutional network (TCN) and multi-head self-attention (MSA) model to predict the RUL of rolling bearings in view of the complex nonlinearity and complexity of mechanical equipment systems. Li et al. [29] combined CNN and LSTM neural network to predict RUL of aeroengines. Xia et al. [30] integrated time series and self-attention network, proposed the distance self-attention network (DSAN) to predict RUL for aeroengines. Al-Dahidi et al. [31] gave RUL prediction of high-reliability equipment based on long short-term memory and MSA. However, the above RUL prediction methods based on deep learning use point estimation, without considering the uncertainty of prediction results. The purpose of RUL prediction is to assist maintenance personnel in making scientific maintenance decisions. Then the RUL prediction methods still need to be further improved.

The degradation process of complex systems inevitably suffer from uncertainty, such as the sensor noise, model structure, model parameters, etc. Therefore, the RUL prediction methods using point estimation are unsuitable for making maintenance decisions while considering risks, since risk is usually measured through uncertainty. The uncertainty quantification in RUL prediction mainly depend on statistical model-based methods, such as Gaussian process regression [32], hidden Markov model [33], etc. Only a few researchers have paid attention to uncertainty quantification of RUL prediction results based on machine learning in recent years. For instance, Li et al. [34] formulated a novel Bayesian deep learning framework to characterize the prognostic uncertainties. Zhao et al. [35] proposed a Li-ion RUL prediction method combining LSTM and Gaussian process regression. Keshun et al. [36] propose a RUL prediction method based on Gamma stochastic process combined with particle filter expectation maximization method and Sparrow Search algorithm optimized SVR to predict the RUL. Zeng and Liang [37] used the deep Gaussian process to

give RUL probabilistic prediction. The RUL probability prediction methods mentioned in the above literature, whether based on statistical models or machine learning, requires the assumption that the prediction results follow a specific distribution. Unfortunately, the distribution of most prediction results does not match a suitable distribution function.

As a non-parametric prediction framework based on deep learning, MQ-RNN doed not need to make assumptions about the distribution of predicted results in advance, which provide a probabilistic multi-step time series regression method to predict the future state [38]. In order to improve the prediction accuracy of RUL and quantify uncertainty of the prediction results, this article proposes a novel non-parametric RUL prediction framework based on XGBoost and MQ-RNN. The main contributions of this article are given as follows:

- A novel non-parametric RUL prediction framework is proposed based on XGBoost and MQ-RNN, which is robust since it does not make any assumptions about the distribution of predicted results. Specifically, XGBoost is used to feature selection, and MQ-RNN is applied to RUL prediction. The proposed method can not only further improve prediction accuracy, but also can quantify uncertainty of the prediction results.
- The article is the first to use MQRNN for RUL prediction. MQ-RNN returns the condition quantile of the predicted RUL distribution by using quantile regression, which adopts direct multi-horizon strategy to avoid error accumulation and maintains efficiency by sharing parameters. In addition, the forking-sequences training scheme in MQ-RNN trains the network model by traversing the data sequences at all time points, which significantly improves the stability and performance of the prediction model.
- The proposed framework is verified by C-MAPSS dataset. Then comparative experiments are conducted. The experimental results show that the proposed method maintains good predictive performance in both point estimation and interval estimation.

The rest of this article is arranged as follows. Section II introduces the basic theory of LSTM and MLP. Section III proposes the RUL prediction framwork based on XGBoost and MQ-RNN. Section IV verifies the proposed framework by C-MAPSS dataset. Section V conducts the comparative experiments. Section VI summarizes this article and states the future research work.

II. BASIC THEORY OF LSTM AND MLP

A. LSTM

LSTM has added gate logic control unit, which effectively solves the problems of gradient explosion and gradient disappearance in the process of long-term sequence training, and makes long-distance time series information more widely used. The structure of the LSTM model is shown in figure 1.

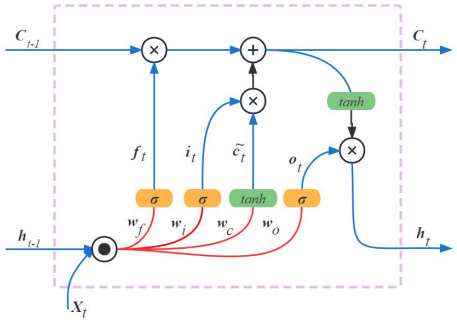

FIGURE 1. The structure of the LSTM model.

The gate control unit mainly consists of three logic control units: forget gate, input gate and output gate. These three logic control units control the three stages of LSTM by setting weights, respectively. The formula of forget gate, input gate and output gate are

$$f_t = \sigma(W_f \cdot [h_{t-1}, x_t] + b_f), \tag{1}$$

$$i_t = \sigma(W_i \cdot [h_{t-1}, x_t] + b_i) \tag{2}$$

and

$$o_t = \sigma(W_o \cdot [h_{t-1}, x_t] + b_o), \tag{3}$$

where x_t is the input data, h_{t-1} is the hidden state of the last moment, W_f, W_i and W_o are the weight matrices in each gated cell, b_f, b_i and b_o are the biases.

The update of cell state in LSTM can be described by

$$\tilde{C}_t = tanh(W_c \cdot [h_{t-1}, x_t] + b_c) \tag{4}$$

and

$$C_t = f_t * C_{t-1} + i_t * \tilde{C}_t, \tag{5}$$

where C_t is the cell state at time t, C_{t-1} is the cell state at time $t-1$, $\tilde{C}_t$ is the candidate vector to add to the cell state, W_c indicates the weight matrix of tanh activation function layer and b_c is the bias. Finally, an output gate and a tanh function layer were used to generate the cell network output h_t, which can be expressed by

$$h_t = o_t * tanh(C_t). \tag{6}$$

B. MLP

Multi-Layer Perceptron (MLP) is mainly composed of input layer, hidden layer and output layer. Hidden layer can have many layers, and the simplest MLP hidden layer only has one layer, as shown in figure 2.

Each layer of the multi-layer perceptron is fully connected. The input layer is used to receive data, the middle layer is used to calculate data, and the output layer is used to output results. In the multi-layer perceptron, the output of the hidden layer will be converted by activation function. The activation function used by MLP in the MQ-RNN prediction

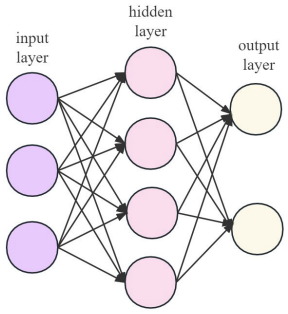

FIGURE 2. The structure of the MLP model.

model is the ReLU activation function. The formula of ReLU activation function is

$$ReLU(x) = max(x, 0). \tag{7}$$

Compared with Sigmoid activation function and Tanh activation function, ReLU activation function solves the problem of gradient disappearance. Moreover, ReLU activation function has only a linear relationship, which is faster than Sigmoid activation function and Tanh activation function in both forward and back propagation.

III. RUL PREDICTION FRAMEWORK BASED ON XGBOOST AND MQ-RNN

In this section, a novel non-parametric RUL prediction framework is proposed to improve the RUL prediction accuracy and quantify the uncertainty of the prediction results. The structue of the framework is shown in Figure 3, which involves three parts: data preprocessing, RUL prediction model construction and RUL prediction.

The data preprocessing mainly includes important feature selection and data normalization. The XGBoost method is used for feature selection to eliminate redundant features. For data normalization, if only single operating conditions are included, data standardization can be directly carried out; if the data collected by the sensor involves multiple operating conditions, it is necessary to cluster the data first, and then standardize it based on the clustering results. Then the RUL prediction model is constructed by using MQ-RNN directly. Input the normalized training set into the MQ-RNN model and train the MQ-RNN model. So the RUL prediction model is obtained by optimizing the parameters in MQ-RNN. Finally, test set is input into the trained RUL prediction model to obtain the RUL prediction results.

A. FEATURE SELECTION

XGBoost is used for feature selection, which is an ensemble learning algorithm based on decision tree and designed for speed and performance. The purpose of the XGBoost is to achieve the effect of a strong classifier by integrating various weak classifiers. By analyzing multidimensional features through XGBoost, the importance of features can be obtained, and the input data is filtered by the importance of

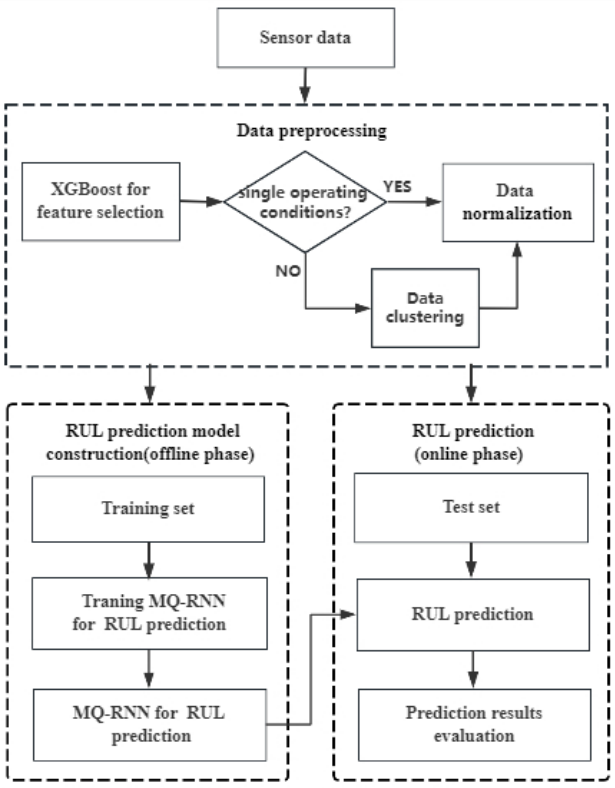

FIGURE 3. The RUL prediction framework.

the features. The basic principles of XGBoost can be found in the literature [39].

For a dataset with n example and m features $D = \{(\mathbf{x}_i, y_i)\}$, $(|D| = n, \mathbf{x}_i \in \mathbf{R}^m, y_i \in \mathbf{R})$, a tree ensemble model uses K additive functions to predict the output

$$\widehat{y}_i = \phi(\mathbf{x}_i) = \sum_{k=1}^{K} f_k(\mathbf{x}_i), f_k \in \mathbf{F}, \tag{8}$$

where $\mathbf{F} = \{f(\mathbf{x}) = \omega_{q(\mathbf{x})}\}$, $(q : \mathbf{R}^m \to T, \omega \in \mathbf{R}^T)$ is the space of regression trees. q is the structure of each tree that maps the dataset to the corresponding leaf weight. T is the number of leaves in the tree. The model is optimized by using the following objective function

$$\mathcal{L} = \sum_i loss(y_i, \hat{y}_i) + \sum_k \Omega(f_k(\mathbf{x}_i)), \tag{9}$$

in which $\Omega(f_k(\mathbf{x}_i)) = \gamma T + \frac{1}{2}\lambda\|\omega_{q(\mathbf{x}_i)}\|^2$ is regularization item, γ and λ are regularization coefficients.

For each iteration of the model, the objective function of the previous iteration will be optimized. The predicted value for tth iteration is

$$\hat{y}_i^{(t)} = \hat{y}_i^{(t-1)} + f_t(\mathbf{x}_i). \tag{10}$$

The objective function $\mathcal{L}$ can transfer to

$$\mathcal{L} = \sum_i loss(y_i, \hat{y}_i^{(t-1)} + f_t(\mathbf{x}_i)) + \Omega(f_t(\mathbf{x}_i)). \tag{11}$$

To minimize the objective function, expand the second-order Taylor expansion of $f_t(\mathbf{x}_i)$ in equation (11) and remove the constant term,

$$\widetilde{\mathcal{L}} \approx \sum_i (loss(y_i, \hat{y}^{(t-1)}) + g_i f_t(\mathbf{x}_i) + \frac{1}{2} h_i f_t^2(\mathbf{x}_i)) + \Omega(f_t(\mathbf{x}_i))$$
$$= \sum_i (g_i f_t(\mathbf{x}_i) + \frac{1}{2} h_i f_t^2(\mathbf{x}_i)) + \Omega(f_t(\mathbf{x}_i)), \quad (12)$$

in which $g_i = \partial_{\hat{y}^{(t-1)}} loss(y_i, \hat{y}_i^{(t-1)})$ and $h_i = \partial^2_{\hat{y}^{(t-1)}} loss(y_i, \hat{y}_i^{(t-1)})$. Let $I_j = \{i \mid q(\mathbf{x}_i) = j\}$ be the set of leaf j. Bring Ω into equation (12), then

$$\widetilde{\mathcal{L}} = \sum_i (g_i f_t(\mathbf{x}_i) + \frac{1}{2} h_i f_t^2(\mathbf{x}_i)) + \gamma T + \frac{1}{2}\lambda \sum_j \omega_j^2$$
$$= \sum_j [(\sum_{i \in I_j} g_i)\omega_j + \frac{1}{2}(\sum_{i \in I_j} h_i + \lambda)\omega_j^2] + \gamma T. \quad (13)$$

Minimize equation (13) to obtain feature importance,

$$\omega_j^* = -\frac{\sum_{i \in I_j} g_i}{\sum_{i \in I_j} h_i + \lambda}. \quad (14)$$

Bring ω_j^* into equation (13), then

$$\widetilde{\mathcal{L}}^* = -\frac{1}{2} \sum_j \frac{(\sum_{i \in I_j} g_i)^2}{\sum_{i \in I_j} h_i + \lambda} + \gamma T. \quad (15)$$

B. DATA NORMALIZATION

Normalization is to limit the pre-processed data to a fixed range such as [0,1] or [-1,1], so as to avoid a series of troubles caused by the singular sample data.

If the dataset under a certain operating condition, the Min-Max normalization method is used and the original data is normalized to the range [0,1] by using linear transformation of the original data, i.e.,

$$x^* = \frac{x - x_{min}}{x_{max} - x_{min}}, \quad (16)$$

where x_{max} and x_{min} are the maximum and minimum values of sample data, respectively.

If the dataset contains a variety of operating conditions, it is necessary to use clustering algorithm first, and then normalize the clustering results by

$$x^i = \frac{x^{i,k} - m^{i,k}}{v^{i,k}}, \quad (17)$$

where k is the number of clusters, the value of k is usually consistent with the type number of operating conditions, $x^{i,k}$ is the data collected by the ith sensor under the kth operating condition, $m^{i,k}$ and $v^{i,k}$ are the mean value and the variance of the original measurement values of the ith sensor under the kth operating condition, respectively.

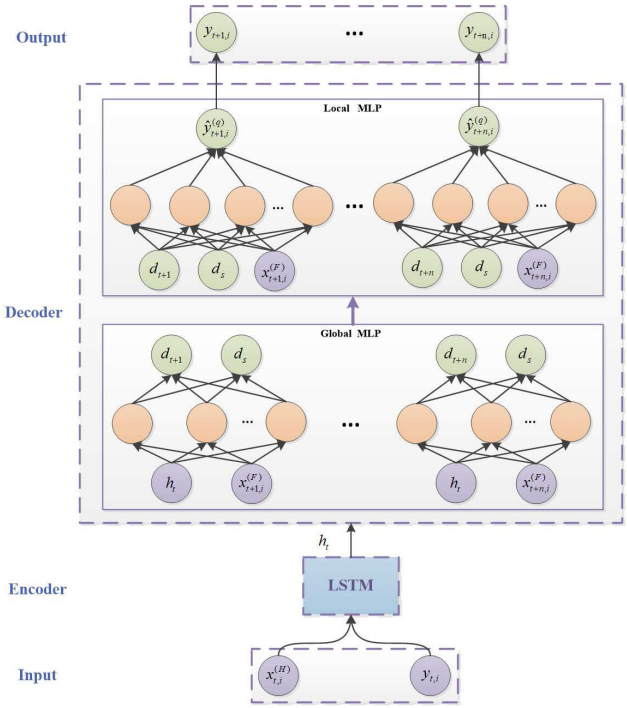

FIGURE 4. The structure of MQ-RNN.

C. RUL PREDICTION MODEL CONSTRUCTION

MQ-RNN is appiled for RUL prediction model construction. The structure of MQ-RNN is encoder-decoder structure, which is shown in Figure 4. MQ-RNN uses LSTM to encode all historical information into hidden states, and designs two MLPs as decoder: a global MLP and a local MLP. The MQ-RNN can deal with the large scale time series regression problem

$$P(y_{t+n,i}, \ldots, y_{t+1,i} \mid y_{:t,i}, x_{:t,i}^{(H)}, x_{t:,i}^{(F)}, x_i^{(S)}), \quad (18)$$

where $y_{\cdot,i}$ is the ith time series to predict, $x_{:t,i}^{(H)}$ are the temporal covariates available in history, $x_{t:,i}^{(F)}$ are the temporal covariates in the future, and $x_i^{(S)}$ are time-invariant features.

Specifically, the input information of the encoder is $x_{:t,i}^{(H)}$ and $y_{:t,i}$, and the hidden state h_t is output after LSTM encoding. In the decoder, the global MLP and the local MLP are used. The input of the global MLP is the hidden state h_t and future input $x_{t:,i}^{(F)}$. The output is $d_{t+N}, N = 1, 2, \ldots, n$ and d_s, where $d_{t+N}, N = 1, 2, \ldots, n$ are the captured information at n future points, and d_s is independent of time and used to capture the global information. The output of global MLP can be expressed by

$$(d_{t+1}, \ldots, d_{t+n}, d_s) = M_g(h_t, x_{t:,i}^{(F)}), \quad (19)$$

in which $M_g(\cdot)$ is the global MLP and the output $d_{(\cdot)}$ can have arbitrary dimension.

The local MLP can respond well to the periodicity of the data and some abrupt changes in the data, which is used to each specific horizon. The input of the local MLP is the future

input $x_{t:,i}^{(F)}$ and the output of global MLP, i.e., $d_{t+N}, N \in \{1, 2, \ldots, n\}$ and d_s. The output of the local MLP is all the required quantiles for the specific future time step

$$(\hat{y}_{t+N,i}^{(q_1)}, \ldots, \hat{y}_{t+N,i}^{(q_Q)}) = M_l(d_{t+N}, d_s, x_{t:,i}^{(F)}), \quad N = 1, 2, \ldots, n, \tag{20}$$

in which $M_l(\cdot)$ is the local MLP and $q_{(\cdot)}$ denotes each of the Q quantiles.

Quantile regression fits different quantiles of the target value by giving different loci. The prediction model is trained by minimizing the the quantile loss function

$$L_q(y, \hat{y}) = q(y - \hat{y})_+ + (1 - q)(\hat{y} + y)_+, \tag{21}$$

where y is the actual value, $\hat{y}$ is the predicted value, q is the quantile coefficient, and $(\cdot)_+ = max(0, \cdot)$.

The MQ-RNN prediction model is trained by minimizing the total quantile loss, namely,

$$L_{total} = \sum_t \sum_q \sum_N L_q(y_{t+N}, \hat{y}_{t+N}^{(q)}). \tag{22}$$

The difference between MQ-RNN and other Seq2Seq architecture models is that it uses the forking-sequences training scheme to improve its performance. Many time series prediction models use a moving-window scheme to cut the time series into subsequences, known as cut-sequences, but a large amount of data needs to be extended in the moving-window scheme. In the MQ-RNN prediction method, the moving-window scheme is not necessary since the forking-sequences training scheme is applied. The forking-sequences training scheme treats each time series of any length as a single sample, which eliminates the need for a large amount of data in the experiment and significantly reduces training time. In addition, the forking-sequences training scheme utilizes all available information at one time to make the model more stable.

IV. VERIFICATION

A. DATASET DESCRIPTION

To validate the effectiveness of the proposed method, the NASA's turbofan engine degradation dataset is considered. The dataset has been generated by commercial modular aero-propulsion system simulation (C-MAPSS), which is a model-based simulation program developed by NASA. The turbofan engine includes five main components, namely, the fan, high-pressure turbine, high-pressure compressor, low-pressure turbine and low-pressure compressor, the states and operating condition of which are observed by 21 sensors that measure features (temperature, pressure, fan speed, etc) in several engine parts during each operation cycle. The turbofan engine is considered to be in a healthy state initially, and the degradation caused by an artificial fault progresses until a system failure occurs.

The C-MAPSS dataset includes four subdatasets collected in various degradation scenarios, denoted by "FD001", "FD002", "FD003" and "FD004", respectively. "FD001" and "FD002" are affected only by high-pressure compressor fault, while "FD003" and "FD004" are subject to high-pressure compressor and fan faults; "FD001" and "FD003" under one operational condition, while "FD002" and "FD004" under multiple operational conditions. Due to subdatasets "FD001" and "FD004" represent the simplest and the most complex situations, they are usually selected for experimental verification. The description of subdatasets "FD001" and "FD004" is shown in Table 1. Each subdataset contains three .txt files, recording training set data, test set data and RUL data, respectively.

TABLE 1. Description of the four subdatasets.

Subdataset	FD001	FD004
Engine number	100	249
Number of operating conditions	1	6
Types of Faults	1	2
Cycle Time	362	543
Data volume	17731	57522

B. DATA PREPROCESSING

In subdatasets "FD001" and "FD004", some sensor measurement data are always constant, which are not valuable in the RUL prediction. In addition, some unimportant features need to be removed to ensure the efficiency of RUL prediction. The XGBoost is used to evaluate the importance of features since it increases the interpretability of the RUL prediction model. Figure 5 shows the feature importance in subdatasets "FD001" and "FD004", and ranks them accordingly. Only important features are selected as RUL prediction model inputs. In subdataset "FD001", the data of sensors 11, 4, 9, 12, 7, 14, 13, 15, 8, 21, 2, 20, and 17 are selected, and in subdataset "FD004", the data of sensors 13, 11, 15, 7, 12, 4, 8, 2, 10, 14, 9, 6, 3 and operating condition 1, 2 are selected. It is easy to see that in "FD001" and "FD004", the importance of different sensor data in the residual life prediction task is different, and the operating condition of the "FD004" also affects the selection of features.

For subdataset "FD001", the Min-Max normalization method is used by formula (16). For subdataset "FD004", k-means algorithm is used for clustering first, then formula (17) is appiled for normalization. Since full life cycle data in C-MAPSS dataset are available, according to literature [40], the true RUL is defined as

$$RUL = \begin{cases} RUL, & if \quad RUL < RUL_{max} \\ RUL_{max}, & if \quad RUL \geq RUL_{max}. \end{cases} \tag{23}$$

C. RUL PREDICTION RESULTS FOR AEROENGINES

In order to select the optimal training model, the Adam optimizer is used to determine the hyperparameters. It determined that the network structure of MQ-RNN has a 3-layer LSTM encoder with 40 LSTM units in each layer, and both global MLP and locall MLP have 2 layers and 20 neuron nodes in

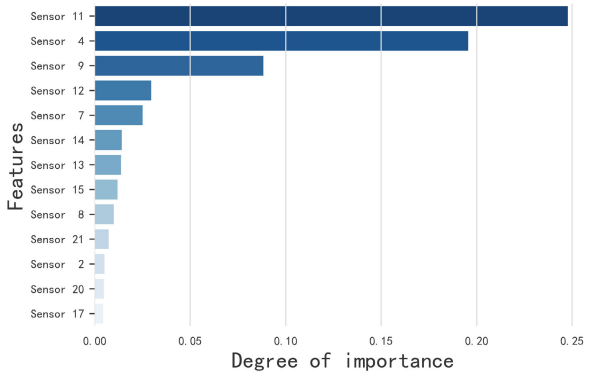

(a) The feature importance in subdataset "FD001"

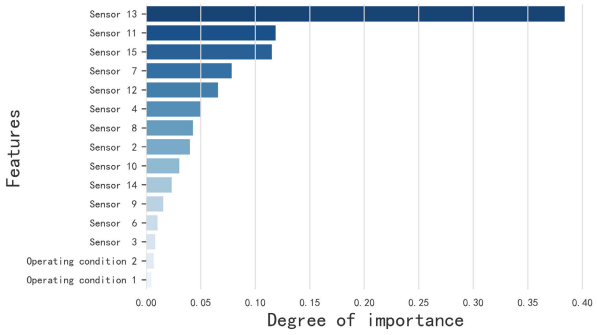

(b) The feature importance in subdataset "FD004"

FIGURE 5. **The feature importance ranking.**

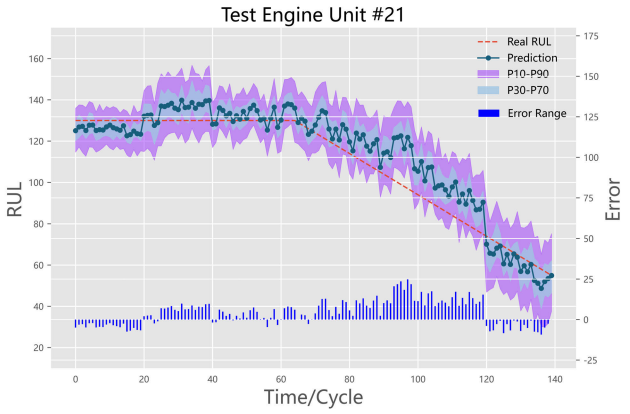

(a) The 21th test engine in dataset FD001

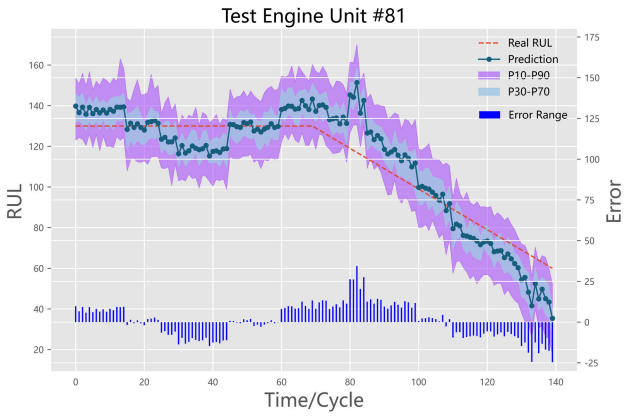

(b) The 81th test engine in dataset FD004

FIGURE 6. **The RUL prediction results for the test engines.**

each layer. The initial learning rate is set to 0.001 for training the model. Then the RUL prediction model is trained.

Input the test set of subdatasets "FD001" and "FD004" into the trained RUL prediction model to obtain the RUL prediction results. Select the representative prediction results randomly, as shown in Figure 6. Specifically, set the predicted point value as the quantile point. The prediction range of 30th to 70th quantile and the prediction range of 10th to 90th quantile are given, respectively. In addition, the RUL prediction errors are also presented in Figure 6 to show the performance of the proposed method.

For inverval prediction, the range of prediction results can roughly represent the uncertainty of prediction results, that is, the larger the range of prediction results, the higher the uncertainty, and the smaller the range of prediction results, the lower the uncertainty. As shown in Figure 6 (a), for 21th engine in subdataset "FD001", the RUL prediction interval for cycles 0 to 20 is narrow, indicating relatively low uncertainty in RUL prediction results, while the RUL prediction interval for cycles 20 to 40 is wide, indicating relatively high uncertainty in RUL prediction results. For the cycles of 40 to 60, the RUL prediction range narrows again, which implies that the uncertainty does not increase as the prediction time point approaches the failure time. As shown in Figure 6 (b), although both the operating conditions and the faults types of the engine increase, the predicted result interval does not significantly increased, which indicates that uncertainty has not increased as time goes on. However, the average prediction interval of subdataset "FD004" is higher than that of subdataset "FD001", as the increase in fault types and operating conditions in the dataset leads to increased uncertainty. For point prediction, both subdatasets "FD001" and "FD004" have no significant cumulative error in the prediction results. In addition, the absolute average error of subdatasets "FD004" is higher than "FD001" since the fault types and operating conditions increase.

V. COMPARATIVE EXPERIMENTS

A. EVALUATION INDICES FOR PREDICTION RESULTS

Firstly, root mean square error (RMSE) and score function (SF) defined in Chen et al. [41] are used to evaluate the point prediction results. RMSE is used to calculate the error between the real RUL and the predicted RUL, which defined as

$$RMSE = \sqrt{\frac{1}{N}\sum_{i=1}^{N}(Y_i - \hat{Y}_i)^2}, \tag{24}$$

where Y_i and $\hat{Y}_i$ represent predicted results and actual values, respectively, and N represents the number of samples of the test set.

SF is used to measure the prediction ability of the model and defined as

$$Score = \sum_{i=1}^{N} s_i = \begin{cases} e^{\frac{\hat{Y}_i - Y_i}{13}}, & if\ Y_i - \hat{Y}_i < 0 \\ e^{\frac{Y_i - \hat{Y}_i}{13}}, & if\ Y_i - \hat{Y}_i \geq 0, \end{cases} \tag{25}$$

where s_i records the scoring result of the final data point of test engine i.

In order to evaluate the prediction results of interval estimation, prediction interval coverage probability (PICP), prediction interval normalized average width (PINAW) and coverage width-based criterion (CWC) defined in Chen et al. [41] are used in this article.

PICP determines whether RUL_i is between the lower bound D_i^σ and the upper bound U_i^σ of the prediction interval under the confidence level $100(1-\sigma)\%$. The PICP is defined as

$$PICP = \frac{1}{N} \sum_{i=1}^{N} \lambda^i_{\{D_i^\sigma \leq RUL_i \leq U_i^\sigma\}}, \tag{26}$$

in which $\lambda^i_{\{\cdot\}}$ is the indicator function, i.e., its value is 1 if the condition $\{\cdot\}$ is met, and 0 if not. The higher the PICP, the better the prediction effect.

PINAW evaluates the prediction ability by calculating the mean breadth of the prediction interval. PINAW is defined as

$$PINAW = \frac{1}{RN} \sum_{i=1}^{N} (U_i^\sigma - D_i^\sigma), \tag{27}$$

where R is the range of RUL_i in the whole prediction period. The lower the PINAW, the better the prediction effect.

The indicator CWC combines PICP and PINAW to provide a comprehensive evaluation score, which can be expressed by

$$CWC = PINAW(1 + \gamma(PICP)e^{-\tau(PICP-\kappa)}), \tag{28}$$

where $\gamma(PICP) = 0$ if $PICP \geq \kappa$, and $\gamma(PICP) = 1$ otherwise, τ and κ are the hyper parameters. Usually, τ ranging from 10 to 100, κ is equal to the confidence level $100(1-\sigma)\%$. The lower the CWC, the better the prediction effect.

B. COMPETITIVE RESULTS COMPARED WITH OTHER PREDICTION METHODS

The median points of the prediction results are regarded as point estimation results, which are compared with the prediction results of SVM [42], MLP [42], NN [2], LSTM [42], DBN [42], MONBNE [23], LSTM-attention [23], MCLSTM-attention-handscraft feature [23] and BiGRU-MMOE [43] models. The evaluation indices RMSE and SF are used to evaluate the predictive performance of point estimation, and the comparison results are shown in Table 2. It is easy to see that RMSE and SF of the proposed method are superior to the above nine prediction methods, which shows that the proposed method has better prediction ability in point prediction.

Compare the evaluation indices of the proposed method with those of the other nine methods that perform better. For subdataset "FD001", the RMSE of the proposed method has decreased by 1.50% compared to BiGRU-MMOE prediction method, and the SF of the proposed method has decreased by 4.31% compared to MCLSTM-attention-handscraft feature prediction method. For subdataset "FD004", the RMSE of the proposed method has decreased by 0.87% compared to BiGRU-MMOE prediction method, and the SF of proposed method has decreased by 22.84% compared to MCLSTM-attention-handscraft prediction method.

TABLE 2. Comparison results of RUL prediction point estimation for different methods.

Method	FD001		FD004	
	RMSE	SF	RMSE	SF
SVM	40.72	7703	59.96	141122
MLP	16.78	560.59	30.96	10444
NN	14.80	496.30	25.80	20422
LSTM	16.14	338	28.17	5550
DBN	15.21	417.59	29.88	7954
MONBNE	15.04	334.23	28.66	6557.62
LSTM-attention	14.53	322.44	27.08	5649.14
MCLSTM-attention -handscraft feature	13.71	[315]	23.81	[4826]
BiGRU-MMOE	[13.22]	-	[18.38]	-
Proposed method	**13.01**	**301.41**	**18.22**	**3723.59**

For interval prediction performance evaluation, the existing interval prediction models MVE [44], Bayesian [44], Bootstrapped SVR [45], IG-MLP [41] and DAE-LSTMQR [41] are selected to compare with the proposed method, and PICP, PINAW and CWC are the evaluation indices. The confidence coefficient σ is set to 0.1, τ and κ are set to 50 and 0.9, respectivly. The comparison results of interval estimation are shown in Table 3. It can be seen that the indices PICP, PINAW and CWC of the proposed method are superior to those of the other five methods.

For subdataset "FD001", the PICP index of the proposed model is 0.97, which is higher than that of the other five interval prediction models. In addition, compared to the DAE-LSTMQR prediction method with better predictive performance among the other five interval prediction models, the PICP index has improved by 2.1%. The indices PINAW and CWC of the proposed model are both 0.34, which are lower than those of the other five prediction models. Both PINAW and CWC have improved by 2.9% compared to those of the DAE-LSTMQR prediction method. For subdataset "FD004", the PICP index of the proposed method is 0.93, which is much higher than the other five interval prediction models and has 7.0% improvement compared to the DAE-LSTMQR prediction method. The indices PINAW and CWC of the proposed method are both 0.55, which are lower than those of the other five interval prediction models. The PINAW has improved by 9.84% compared to that of the Bayesian prediction method, and the CWC has improved by 46.1% compared to that of the DAE-LSTMQR prediction method.

TABLE 3. Comparison results of RUL prediction interval estimation of different methods.

Method	FD001			FD004		
	PICP	PINAW	CWC	PICP	PINAW	CWC
MVE	0.82	0.43	100.49	0.74	1.02	136.64
Bayesian	0.92	0.39	7.99	0.81	[0.61]	29.57
Bootstrapped SVR	0.93	0.41	1.52	0.82	0.64	5.88
IG-MLP	0.8	0.39	705.53	0.68	0.72	943.75
DAE-LSTMQR	[0.95]	[0.35]	[0.35]	[0.87]	1.02	[1.02]
Proposed method	**0.97**	**0.34**	**0.34**	**0.93**	**0.55**	**0.55**

In summary, whether it is a dataset with a single operating condition and a single fault type, or a dataset with multiple operating conditions and multiple fault types, the method proposed in this article maintains good predictive performance in both point estimation and interval estimation.

C. DISCUSSION ON INTERVAL PREDICTION VERSUS POINT PREDICTION

In the field of RUL prediction, the prediction results have a certain degree of uncertainty. Compared to the determined RUL point prediction, interval prediction has the following advantages:

- Interval prediction can effectively quantify uncertainty, and the interval width of the predicted results at a certain confidence level can characterize the level of uncertainty. When the width of the prediction interval is wide, the uncertainty of the prediction result is high. When the width of the prediction interval is narrow, the uncertainty of the prediction result is low.
- The interval prediction of RUL can help equipment maintenance personnel make reasonable maintenance decisions considering reliability or risk, but the point prediction of RUL cannot. For example, as shown in Figure 6 (a), the RUL point prediction during cycle range $[70, 90]$ of the 21th engine in subdataset "FD001" is inaccurate. If there has no additional information available, it may lead to incorrect maintenance decisions. If interval estimation results are available, maintenance will be carried out in advance. Therefore, the RUL prediction interval estimation results under different confidence levels has practical significance for maintenance decision-making, the results of which can be used as supplementary information combined with point prediction to enhance the stability and effectiveness of the decision-making.

VI. CONCLUSION

In order to improve the RUL prediction accuracy and quantify uncertainty of prediction results, a novel non-parametric RUL prediction framework based on XGBoost and MQ-RNN is proposed in this article. The framework uses XGBoost to select important features, and applied MQ-RNN to prediction RUL. Then the proposed RUL prediction framework is verified by C-MAPSS dataset, and the RUL prediction results of point estimation and interval estimation are given, respectively. The comparative experimental results show that whether a dataset with a single operating condition and a single fault type, or a dataset with multiple operating conditions and multiple fault types, the proposed method maintains good predictive performance in both point estimation and interval estimation. The proposed method can quantify the uncertainty of RUL prediction results to provide risk assessment values, and assist personnel in equipment maintenance support to make scientific maintenance decisions while considering risks.

The proposed method mainly includes two limitations:

- High computational complexity: The MQ-RNN model has high computational complexity, especially when dealing with long sequences or high-dimensional data. Since the MQ-RNN model needs to estimate multiple quantiles at each time step, a lot of computation is required. This can cause the training and inference process to become time consuming and require greater computational resources.
- High data requirements: MQ-RNN model has high requirements for training data. Since the MQ-RNN model needs to estimate multiple quantiles, there needs to be enough samples in the training data to cover the target quantile. If the distribution of training data is not uniform or there is a lack of representative samples, it may lead to poor performance of the MQ-RNN model on some quantiles.

In summary, in the future, we will focus on the construction of lightweight models for predicting RUL. In addition, when the data is not sufficient, we can enhance the data by generating adversarial networks and predict the RUL on the generated new dataset.

DATA AVAILABILITY STATEMENT

The data that support the findings of this study are available at https://www.nasa.gov/intelligent-systems-division.

ACKNOWLEDGMENT

The authors would like to thank all the anonymous reviewers for their insightful comments.

REFERENCES

[1] H. Shao, J. Lin, L. Zhang, D. Galar, and U. Kumar, "A novel approach of multisensory fusion to collaborative fault diagnosis in maintenance," *Inf. Fusion*, vol. 74, pp. 65–76, Oct. 2021.

[2] X. Li, Q. Ding, and J.-Q. Sun, "Remaining useful life estimation in prognostics using deep convolution neural networks," *Rel. Eng. Syst. Saf.*, vol. 172, pp. 1–11, Apr. 2018.

[3] F. Cheng, L. Qu, and W. Qiao, "Fault prognosis and remaining useful life prediction of wind turbine gearboxes using current signal analysis," *IEEE Trans. Sustain. Energy*, vol. 9, no. 1, pp. 157–167, Jan. 2018.

[4] U. Bhardwaj, A. P. Teixeira, and C. Guedes Soares, "Bayesian framework for reliability prediction of subsea processing systems accounting for influencing factors uncertainty," *Rel. Eng. Syst. Saf.*, vol. 218, Feb. 2022, Art. no. 108143.

[5] Y. Li, Z. Liu, Z. He, L. Tu, and H.-Z. Huang, "Fatigue reliability analysis and assessment of offshore wind turbine blade adhesive bonding under the coupling effects of multiple environmental stresses," *Rel. Eng. Syst. Saf.*, vol. 238, Oct. 2023, Art. no. 109426.

[6] W. Mao, J. He, and M. J. Zuo, "Predicting remaining useful life of rolling bearings based on deep feature representation and transfer learning," *IEEE Trans. Instrum. Meas.*, vol. 69, no. 4, pp. 1594–1608, Apr. 2020.

[7] Y. Lei, N. Li, L. Guo, N. Li, T. Yan, and J. Lin, "Machinery health prognostics: A systematic review from data acquisition to RUL prediction," *Mech. Syst. Signal Process.*, vol. 104, pp. 799–834, May 2018.

[8] S. Bai, T. Huang, Y.-F. Li, N. Lu, and H.-Z. Huang, "A probabilistic fatigue life prediction method under random combined high and low cycle fatigue load history," *Rel. Eng. Syst. Saf.*, vol. 238, Oct. 2023, Art. no. 109452.

[9] Z. Zhang, X. Chen, E. Zio, and L. Li, "Multi-task learning boosted predictions of the remaining useful life of aero-engines under scenarios of working-condition shift," *Rel. Eng. Syst. Saf.*, vol. 237, Sep. 2023, Art. no. 109350.

[10] Z. He, H. Shao, X. Zhong, and X. Zhao, "Ensemble transfer CNNs driven by multi-channel signals for fault diagnosis of rotating machinery cross working conditions," *Knowledge-Based Syst.*, vol. 207, Nov. 2020, Art. no. 106396.

[11] Z. Xue, Y. Zhang, C. Cheng, and G. Ma, "Remaining useful life prediction of lithium-ion batteries with adaptive unscented Kalman filter and optimized support vector regression," *Neurocomputing*, vol. 376, pp. 95–102, Feb. 2020.

[12] Z. Pan, Z. Meng, Z. Chen, W. Gao, and Y. Shi, "A two-stage method based on extreme learning machine for predicting the remaining useful life of rolling-element bearings," *Mech. Syst. Signal Process.*, vol. 144, Oct. 2020, Art. no. 106899.

[13] J. Wu, X. Cheng, H. Huang, C. Fang, L. Zhang, X. Zhao, L. Zhang, and J. Xing, "Remaining useful life prediction of lithium-ion batteries based on PSO-RF algorithm," *Frontiers Energy Res.*, vol. 10, Jan. 2023, Art. no. 937035.

[14] L. Ren, H. Qin, Z. Xie, B. Li, and K. Xu, "Aero-engine remaining useful life estimation based on multi-head networks," *IEEE Trans. Instrum. Meas.*, vol. 71, pp. 1–10, 2022.

[15] C. Peng, Y. Chen, Q. Chen, Z. Tang, L. Li, and W. Gui, "A remaining useful life prognosis of turbofan engine using temporal and spatial feature fusion," *Sensors*, vol. 21, no. 2, p. 418, Jan. 2021.

[16] L. Guo, Y. Lei, S. Xing, T. Yan, and N. Li, "Deep convolutional transfer learning network: A new method for intelligent fault diagnosis of machines with unlabeled data," *IEEE Trans. Ind. Electron.*, vol. 66, no. 9, pp. 7316–7325, Sep. 2019.

[17] J. Ma, H. Su, W.-L. Zhao, and B. Liu, "Predicting the remaining useful life of an aircraft engine using a stacked sparse autoencoder with multilayer self-learning," *Complexity*, vol. 2018, pp. 1–13, Jul. 2018.

[18] R. H. Jiao, K. X. Peng, J. Dong, K. Zhang, and C. Zhang, "A health indicator construction method based on deep belief network for remaining useful life prediction," in *Proc. Prognostics Syst. Health Manage. Conf. (PHMQingdao)*, China, 2019, pp. 1–6.

[19] L. Ren, Y. Sun, H. Wang, and L. Zhang, "Prediction of bearing remaining useful life with deep convolution neural network," *IEEE Access*, vol. 6, pp. 13041–13049, 2018.

[20] L. Guo, N. Li, F. Jia, Y. Lei, and J. Lin, "A recurrent neural network based health indicator for remaining useful life prediction of bearings," *Neurocomputing*, vol. 240, pp. 98–109, May 2017.

[21] N. Ding, H. Li, Z. Yin, N. Zhong, and L. Zhang, "Journal bearing seizure degradation assessment and remaining useful life prediction based on long short-term memory neural network," *Measurement*, vol. 166, Dec. 2020, Art. no. 108215.

[22] S. Behera, R. Misra, and A. Sillitti, "Multiscale deep bidirectional gated recurrent neural networks based prognostic method for complex non-linear degradation systems," *Inf. Sci.*, vol. 554, pp. 120–144, Apr. 2021.

[23] S. Xiang, Y. Qin, J. Luo, H. Pu, and B. Tang, "Multicellular LSTM-based deep learning model for aero-engine remaining useful life prediction," *Rel. Eng. Syst. Saf.*, vol. 216, Dec. 2021, Art. no. 107927.

[24] Y. Qin, J. Zhou, and D. Chen, "Unsupervised health indicator construction by a novel degradation-trend-constrained variational autoencoder and its applications," *IEEE/ASME Trans. Mechatronics*, vol. 27, no. 3, pp. 1447–1456, Jun. 2022.

[25] J. Zhou, Y. Qin, J. Luo, S. Wang, and T. Zhu, "Dual-thread gated recurrent unit for gear remaining useful life prediction," *IEEE Trans. Ind. Informat.*, vol. 19, no. 7, pp. 8307–8318, Jul. 2023.

[26] J. Zhou, Y. Qin, J. Luo, and T. Zhu, "Remaining useful life prediction by distribution contact ratio health indicator and consolidated memory GRU," *IEEE Trans. Ind. Informat.*, vol. 19, no. 7, pp. 8472–8483, May 2023.

[27] J. Li, F. Huang, H. Qin, and J. Pan, "Research on remaining useful life prediction of bearings based on MBCNN-BiLSTM," *Appl. Sci.*, vol. 13, no. 13, p. 7706, Jun. 2023.

[28] G. Jiang, Z. Duan, Q. Zhao, D. Li, and Y. Luan, "Remaining useful life prediction of rolling bearings based on TCN-MSA," *Meas. Sci. Technol.*, vol. 35, no. 2, Feb. 2024, Art. no. 025125.

[29] H. Li, Z. Wang, and Z. Li, "An enhanced CNN-LSTM remaining useful life prediction model for aircraft engine with attention mechanism," *PeerJ Comput. Sci.*, vol. 8, p. e1084, Aug. 2022.

[30] J. Xia, Y. Feng, D. Teng, J. Chen, and Z. Song, "Distance self-attention network method for remaining useful life estimation of aeroengine with parallel computing," *Rel. Eng. Syst. Saf.*, vol. 225, Sep. 2022, Art. no. 108636.

[31] S. Al-Dahidi, M. Rashed, M. Abu-Shams, M. Mellal, M. Alrbai, S. Ramadan, and E. Zio, "A novel approach for remaining useful life prediction of high-reliability equipment based on long short-term memory and multi-head self-attention mechanism, *Qual. Rel. Eng. Int.*, vol. 40, no. 2, pp. 948–969, 2024.

[32] Y. Guo, X. Yu, Y. Wang, and K. Huang, "Health prognostics of lithium-ion batteries based on universal voltage range features mining and adaptive multi-Gaussian process regression with Harris hawks optimization algorithm," *Rel. Eng. Syst. Saf.*, vol. 244, Apr. 2024, Art. no. 109913.

[33] M. Lin, Y. You, W. Wang, and J. Wu, "Battery health prognosis with gated recurrent unit neural networks and hidden Markov model considering uncertainty quantification," *Rel. Eng. Syst. Saf.*, vol. 230, Feb. 2023, Art. no. 108978.

[34] G. Li, L. Yang, C.-G. Lee, X. Wang, and M. Rong, "A Bayesian deep learning RUL framework integrating epistemic and aleatoric uncertainties," *IEEE Trans. Ind. Electron.*, vol. 68, no. 9, pp. 8829–8841, Sep. 2021.

[35] J. Zhao, Y. Zhu, B. Zhang, M. Liu, J. Wang, C. Liu, and Y. Zhang, "Method of predicting SOH and RUL of lithium-ion battery based on the combination of LSTM and GPR," *Sustainability*, vol. 14, no. 19, p. 11865, Sep. 2022.

[36] Y. Keshun, Q. Guangqi, and G. Yingkui, "Remaining useful life prediction of lithium-ion batteries using EM-PF-SSA-SVR with gamma stochastic process," *Meas. Sci. Technol.*, vol. 35, no. 1, Jan. 2024, Art. no. 015015.

[37] J. Zeng and Z. Liang, "A deep Gaussian process approach for predictive maintenance," *IEEE Trans. Rel.*, vol. 72, no. 3, pp. 916–933, Oct. 2023.

[38] R. Wen, K. Torkkola, B. Narayanaswamy, and D. Madeka, "A multi-horizon quantile recurrent forecaster," in *Proc. 31st Conf. Neural Inf. Process. Syst.*, 2017, p. 1711.

[39] T. Chen and C. Guestrin, "XGBoost: A scalable tree boosting system," in *Proc. 22nd ACM SIGKDD Int. Conf. Knowl. Discovery Data Mining*, Aug. 2016, pp. 785–794.

[40] T. Zuo, K. Zhang, Q. Zheng, X. Li, Z. Li, G. Ding, and M. Zhao, "A hybrid attention-based multi-wavelet coefficient fusion method in RUL prognosis of rolling bearings," *Rel. Eng. Syst. Saf.*, vol. 237, Sep. 2023, Art. no. 109337.

[41] C. Chen, J. Shi, M. Shen, L. Feng, and G. Tao, "A predictive maintenance strategy using deep learning quantile regression and kernel density estimation for failure prediction," *IEEE Trans. Instrum. Meas.*, vol. 72, pp. 1–12, 2023.

[42] C. Zhang, P. Lim, A. K. Qin, and K. C. Tan, "Multiobjective deep belief networks ensemble for remaining useful life estimation in prognostics," *IEEE Trans. Neural Netw. Learn. Syst.*, vol. 28, no. 10, pp. 2306–2318, Oct. 2017.

[43] Y. Zhang, Y. Xin, Z.-W. Liu, M. Chi, and G. Ma, "Health status assessment and remaining useful life prediction of aero-engine based on BiGRU and MMoE," *Rel. Eng. Syst. Saf.*, vol. 220, Apr. 2022, Art. no. 108263.

[44] A. Khosravi, S. Nahavandi, D. Creighton, and A. F. Atiya, "Comprehensive review of neural network-based prediction intervals and new advances," *IEEE Trans. Neural Netw.*, vol. 22, no. 9, pp. 1341–1356, Sep. 2011.
[45] I. D. Lins, E. L. Droguett, M. D. C. Moura, E. Zio, and C. M. Jacinto, "Computing confidence and prediction intervals of industrial equipment degradation by bootstrapped support vector regression," *Rel. Eng. Syst. Saf.*, vol. 137, pp. 120–128, May 2015.

YANTAO YIN received the B.S. degree in electrical engineering and automation from Shandong University of Technology, Shandong, China, in 2002, and the M.S. degree in control theory and control engineering from the Naval Aviation Engineering College, Yantai, China, in 2009. He is currently a Lecturer with Naval Aviation University, Yantai. His research interests include equipment reliability and equipment support.

JIANYIN ZHAO received the B.S. degree in applied mathematics, the M.S. degree in management science and engineering, and the Ph.D. degree in control science and engineering from the National University of Defense Technology, Hunan, China, in 1999, 2002, and 2005, respectively. He is currently an Associate Professor with Naval Aviation University, Yantai, China. His research interests include equipment reliability and equipment support.

XIAO ZHANG received the B.S. degree in software engineering from Tianjin University of Science and Technology, Tianjin, China, in 2021, where she is currently pursuing the master's degree. Her research interests include fault prognosis and deep learning.

YING LIU received the B.S. degree in computer science from Tianjin University of Technology, Tianjin, China, in 2004, and the M.S. and Ph.D. degrees in systems engineering from Tianjin University, Tianjin, in 2006 and 2009, respectively. She is currently a Professor with the School of Management, Tianjin University of Technology. Her research interests include prognostics and health management, reliability theory of systems, and decision making under uncertainty.